



ELSEVIER

Journal of Electron Spectroscopy and Related Phenomena 114–116 (2001) 997–1003

JOURNAL OF
ELECTRON SPECTROSCOPY
and Related Phenomena

www.elsevier.nl/locate/elspec

The multidisciplinary of spectromicroscopy: from geomicrobiology to archaeology

Gelsomina De Stasio^{a,*}, B. Gilbert^a, B.H. Frazer^{a,b}, K.H. Nealson^c, P.G. Conrad^c,
V. Livi^d, M. Labrenz^e, J.F. Banfield^e

^aUniversity of Wisconsin, Department of Physics, Madison, WI, USA

^bEcole Polytechnique Federale de Lausanne, Switzerland

^cJet Propulsion Laboratory, California Institute of Technology, Pasadena, CA, USA

^dUniversity of Pennsylvania, Department of Archaeology, Philadelphia, PA, USA

^eUniversity of Wisconsin, Department of Geology and Geophysics, Madison, WI, USA

Received 8 August 2000; received in revised form 22 September 2000; accepted 3 October 2000

Abstract

Synchrotron X-ray PhotoElectron Emission Microscopy (X-PEEM) is a useful tool to investigate the microchemical composition of a variety of different samples, including cells in culture, tissue sections, magnetic material, bacteria, rocks, materials science, tribology and archaeology specimens. The MEPHISTO X-PEEM, installed at the Wisconsin Synchrotron Radiation Center, reached a peak resolution of 20 nm, has been extensively used for the last 4 years to explore all of the above systems. The experiments reported here are some of the most unusual ones for this technique: ZnS precipitating bacteria, Mn and Fe oxide rocks and archaeological coins. The microchemistry of each one of these samples delivered new results. © 2001 Elsevier Science B.V. All rights reserved.

Keywords: X-PEEM; Spectromicroscopy; ZnS precipitating bacteria; Banded iron formation; Roman silver coin

1. Introduction

X-ray PhotoElectron Emission Microscopy (X-PEEM) was originally developed for studying the surface microchemistry of materials science specimens [1–3]. It has then evolved into a valuable tool to investigate the magnetic properties of materials [4] and the microchemistry of cells and tissues [5–7]. Nevertheless, these types of samples are not the only ones that can be explored with X-PEEM. We have

tested the use of the MEPHISTO X-PEEM instrument on a whole variety of different specimens of interest in completely different disciplines. These include liquids confined in an ultra-high vacuum (UHV) compatible sealed cell [8], micro-corrosion on the surface of jet engine components, lubricant films of tribological interest [9,10], thin polymer layers [11], carbon nanowires [12], bacteria and their metabolic byproducts [13,14], rocks containing several elements in micro-localized oxidation states, and archaeological coins. Since none of these systems had previously been studied with this or similar techniques, we obtained, to our surprise and delight, valuable new information from all these systems.

*Corresponding author. Tel.: +1-608-877-2000/2; fax: +1-608-263-0800.

E-mail address: gdestasi@facstaff.wisc.edu (G. De Stasio).

These experiments also had the effect of transforming our group into a truly interdisciplinary one.

The conditions under which a sample is PEEM-detectable are apparently very stringent. The sample must in fact be: (i) a conductor; (ii) UHV compatible; (iii) flat. In reality, each one of these conditions turns out to be quite forgiving. Conductivity was the biggest surprise: a polymer microtomed section as thick as 0.5 μm , or a 1-mm thick rock were conductive enough to generate usable X-PEEM distribution maps and spectra. Note that the samples are kept at high negative voltage (–12 to –18 kV) during a PEEM experiment [15]. In the case of the rock, it is possible that we are observing photoconductivity under X-ray illumination [16], although in the polymer case, this explanation is not acceptable.

The case of UHV compatibility has also been surprising: a very preoccupying event for surface scientists is the introduction of oil in their vacuum chamber. For the tribology experiments, we studied metal coupons that had been immersed in lubricant oil in the presence of additives, at high temperature, high pressure and under mechanical rubbing to simulate car engine stress conditions, and the consequent oil additive film formation. The samples were rinsed in a beaker containing hexanes for a few seconds, and then inserted into the UHV chamber directly. This was not a very thorough cleansing by UHV standards. Nevertheless, the base pressure in the chamber was 10^{-9} Torr or lower, and the results of Refs. [9,10] could be obtained.

On the other hand, when we wanted to analyze wet samples, in the pursuit of the elusive goal of studying living cells, we had to develop a vacuum tight water pocket, that would confine water in UHV for as long as 3.5 days without leaking, before we could acquire X-PEEM spectra [8].

The sample surface flatness constraint is always a concern. A high resistivity sample with a surface corrugation of 1 μm peak-valley can be imaged, but the local electric field when the sample is held at high voltage is strongly inhomogeneous, generating artifact topography in the images.

In some cases, such artifacts can be eliminated via software, but only in elemental distribution maps, normalized to obtain a ‘pure chemistry–no topography map’. Spectra originating from such corru-

gated insulating surfaces may exhibit very strange behavior such as negative peaks in the spectra and edge lensing effects in the images, which we had to analyze and characterize carefully, before any valuable microchemical information could be extracted [17].

Each one of the samples described above presents different challenges for X-PEEM analysis, and sample preparation must be optimized to render the experiment possible. We discuss here three of the unusual X-PEEM experiments in geomicrobiology, geology and archaeology.

1.1. Geomicrobiology

One author (J.F.B.) and coworkers recently discovered that sulfate reducing bacteria are associated with ZnS in biofilms collected from a flooded zinc mine in Southern Wisconsin. They observed that abundant, extracellular, spherical, micron-scale aggregates of nanocrystalline (approximately 2–5 nm diameter) sphalerite (ZnS) are formed in natural biofilms by these sulfate-reducing bacteria. Biofilms concentrate Zn by a factor of about 10^6 relative to the dilute groundwater (0.09–1.1 ppm Zn). DNA analysis of this novel ZnS precipitating bacteria, to determine their phylogeny, identified them as part of the family Desulfobacteriaceae [13]. TEM and diffraction results on the precipitated spheres were consistent with ZnS, based on the interatomic distance and elemental composition, but definite proof that the oxidation state of S was consistent with ZnS was necessary. We therefore analyzed them with MEPHISTO and provided conclusive evidence.

1.2. Geology

Microchemistry of rocks by a technique sensitive to the oxidation state of elements at the microscopic level, such as X-PEEM, is helpful in the characterization and interpretation of the formation of the rock itself. We studied a ~2.0 billion-year-old rock from a manganese deposit, which is part of a banded iron formation (BIF) in the Kalahari Desert in South Africa. The genesis of BIF is uncertain, and one school of thought proposes a biological origin. We decided to study this with MEPHISTO to look for evidence of biogenicity in the form of microchemical

inhomogeneities. We observed no structures consistent with microbial microfossils, nor did we observe any other conclusive evidence of biogenicity. We were able to observe mixed oxidation states of manganese ($\text{Mn}^{2+}/\text{Mn}^{3+}$ and Mn^{4+}) and oxidized iron (Fe^{3+}) [18]. This technique was clearly able to image microchemical inhomogeneity in the rock at fine spatial scales $\sim 0.1 \mu\text{m}$.

1.3. Archaeology

A surface sensitive technique such as X-PEEM is not expected to be the ideal tool to analyze the alloy chemistry of an ancient coin. A bulk sensitive technique such as neutron activation would be much better suited for the goal. Nevertheless, we decided to try and we found unprecedented information: we observed the presence of fluorine in a 211 B.C. Roman silver coin. Fluorine has never been found in silver coins, and we do not know why it was there, and how it was incorporated in the silver alloy, but we were able to rule out the possibility of surface contamination.

2. Experimental

2.1. X-PEEM spectromicroscopy

Extensive descriptions of the MEPHISTO X-PEEM instrument can be found in Refs. [15,19].

2.2. Geomicrobiology

The bacterial biofilm was extracted from the flooded mine ore by SCUBA divers, and stored in vials at -20°C . Samples for MEPHISTO were simply a $5\text{-}\mu\text{l}$ droplet of the mine water and biofilm fragments in suspension, deposited on gold coated silicon substrates, and air dried. The relevant bacteria were identified among many others by their morphology and the presence of the microspheres on their cell bodies [13].

2.3. Geology

The manganese deposit rock sample was collected from the BIF in South Africa by J. Kirschvink

(Caltech). We obtained a small piece of it, cut it, and then polished it by hand with decreasing diameter alumina powders, down to $0.3 \mu\text{m}$. The rock surface after polishing was very inhomogeneous at the visible light microscope, exhibiting shallow $5\text{--}100 \mu\text{m}$ wide ovoid pits, probably because these regions contained softer mineral phases preferentially eroded by polishing. The ovoids were not accessible to X-PEEM because they did not photoemit. We do know from environmental scanning electron microscopy, that the ovoid features contain a variety of manganese oxides and Mn-rich carbonate phases. The rock matrix, mostly manganese and iron oxides, could be imaged and analyzed in MEPHISTO.

2.4. Archaeology

A Roman silver coin (dated 211 B.C.) was first analyzed in MEPHISTO, then also with an XPS system at the US Air Force Base in Dayton, OH, and the study was completed with XPS ESCA-300 Scienta instrument at the EPFL in Switzerland. The results presented here are from the ESCA instrument, although they could technically be obtained with the other two instruments if enough time was available. The ESCA spatial resolution is determined by the X-ray beam size (Al $K\alpha$ rotating anode source, 1486 eV , slit delimited to be $500 \times 500 \mu\text{m}^2$). The coin was vacuum cleaned with trichloroethane, acetone and ethanol in ultrasonic baths for 20 min each, before being inserted in the vacuum systems. XPS spectra were acquired in $5\text{--}10$ locations of the coin surface, then it was sputtered with 5 keV Ar ions for 100 min and analyzed again in $5\text{--}10$ locations.

3. Results and discussion

Fig. 1 top-left shows the direct MEPHISTO micrograph of one of the ZnS precipitating bacteria. The images below are the distribution maps of the sulfide and sulfate on and around the same bacterium. In the sulfide distribution map, two of the sphalerite spheres are visible, not corresponding to a strong sulfate signal in the sulfate distribution map. The top spectrum on the right was extracted from the two regions highlighted in yellow on the image. This spectrum clearly shows the presence of sulfur in two

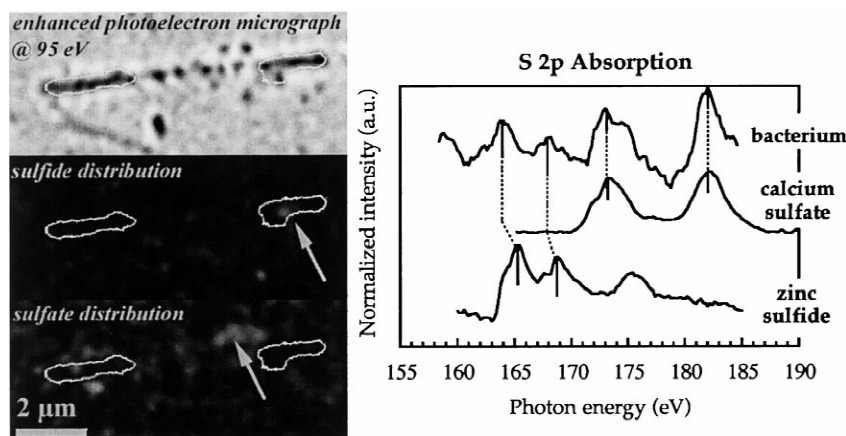


Fig. 1. Direct MEPHISTO micrograph acquired at 95 eV photon energy (top left). Below left the sulfide and sulfate distribution maps, showing higher concentration in lighter gray. The sulfide map was obtained from images taken at 164, 160 and 156 eV, the sulfate map 174, 160 and 156 eV. The regions outlined on the images indicate where the bacterium spectrum on the right was acquired. The spectra on the right show a comparison of XANES on the bacterium and two reference compounds: calcium sulfate and zinc sulfide.

different chemical states, one with main peaks at 174 and 182 eV, interpreted as a sulfate, and one with peaks at 164 and 178 eV, interpreted as sulfide. Spectra from a reference sample of calcium sulfate confirm the sulfate interpretation. The sulfide interpretation is also confirmed by a reference compound, ZnS, although the spectra from the reference have similar lineshapes, their energy position is shifted by 1 eV. This shift does not affect the interpretation of the bacterium spectral peaks at 164 and 178 eV, which can only be attributed to a sulfide. Interestingly, organic and inorganic formation of the same compound might exhibit different spectral behavior. This may be due, for example, to the microstructure of the sphalerite ZnS, formed by 3 nm diameter nanospheres (S.E.M. data, not shown [13]). The surface/volume ratio is therefore unusually large, affecting the XANES peak position.

Fig. 2 shows the distribution maps of Mn^{2+} , $\text{Mn}^{2+}/\text{Mn}^{3+}$ and Fe^{3+} acquired from the BIF rock sample. The large void in region 3 is one of the poorly conducting ovoid features, which did not emit photoelectrons. Iron forms discrete inclusions in the manganese oxide matrix (region 1). The manganese phases are interspersed with different local concentrations. In particular, in region 2, Mn^{2+} is present in higher concentration than $\text{Mn}^{2+}/\text{Mn}^{3+}$. We did not find evidence of biogenicity.

Nevertheless, we determined that the elemental and oxidative microchemistry of this rock can be studied with the necessary sensitivity and spatial resolution with MEPHISTO. Although this particular rock matrix was conductive enough to be detectable with X-PEEM, we cannot assume that every rock would be [20]. It is possible that the insulating Mn oxides in the rock, in fact, become photoconductive once illuminated by X-rays [16]. Alternatively, a high concentration of impurities in the minerals may be doping insulating crystals and increasing their conductivity, although the resistivity should be finite also when the sample is not X-ray illuminated, which is not the case.

Fig. 3 shows the silver coin and the F 1s XPS spectra acquired on it. XPS spectra taken from the coin before sputtering exhibited several contaminants, with a predominance of sulfur, and no F. After sputtering all contaminants were removed (O and S were not detectable), the Ag and F spectral peaks became much more intense. This result indicates that F is in the coin Ag alloy, and not a surface contaminant. As it can be seen in Fig. 3, the coin did not tarnish. Since the presence of the fluorine in silver coins has never been documented, and this coin did not tarnish, we speculate that the two phenomena may be related. We do not know what compound F is forming in the Ag alloy. We analyzed

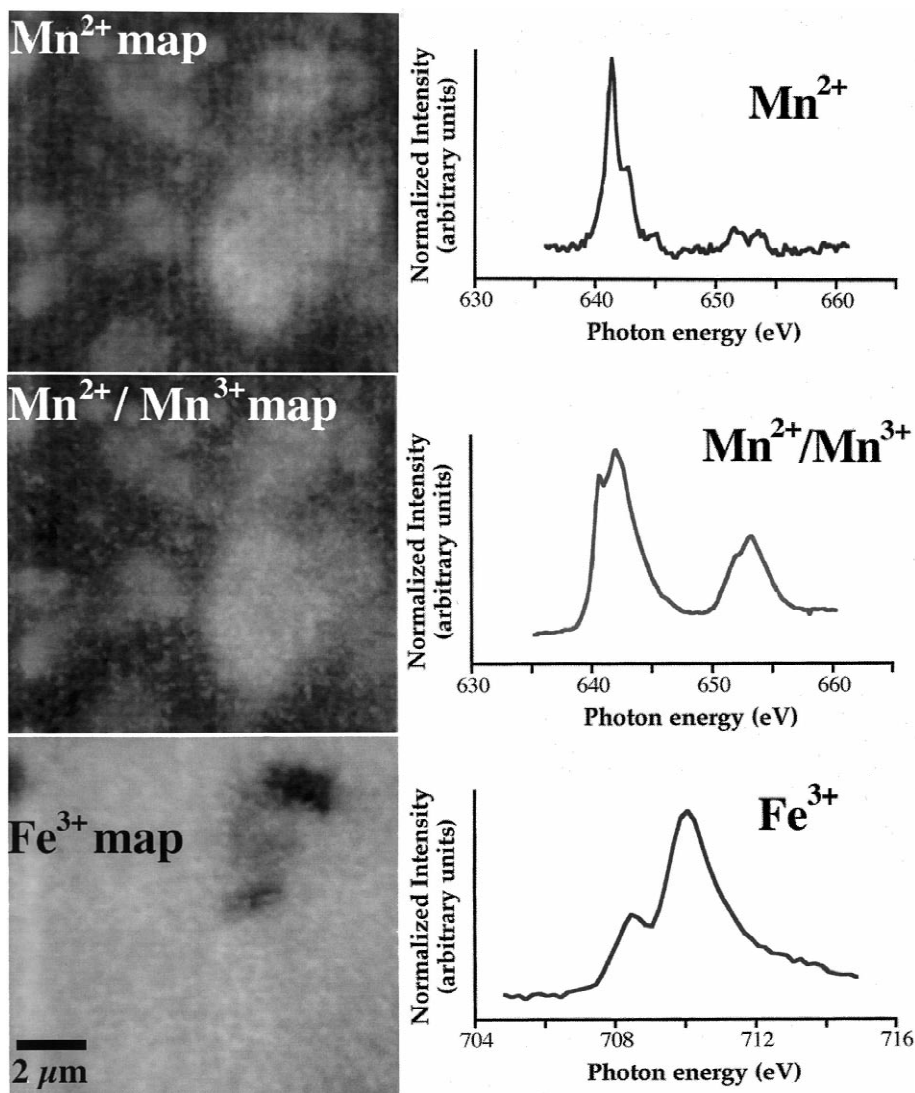


Fig. 2. Left: MEPHISTO distribution maps of Mn^{2+} and $\text{Mn}^{2+}/\text{Mn}^{3+}$ and Fe^{3+} acquired on the Kalahari Desert banded iron formation (BIF). In each map darker pixels correspond to higher concentration of the element. Right: MEPHISTO XANES spectra showing a predominance of Mn^{2+} or $\text{Mn}^{2+}/\text{Mn}^{3+}$, or Fe^{3+} in different locations (1, 2 and 3) on the surface of the rock. Note that the distribution maps of Mn^{2+} and $\text{Mn}^{2+}/\text{Mn}^{3+}$ are similar but not identical. The iron distribution map is completely different.

several possibilities and failed to find a compound that would form at or above the Ag melting point (960°C [21]) and that would not tarnish. The most obvious, AgF is to be ruled out because it turns black in contact with air [21], as AgNO_3 does in photographic emulsion. AgF_2 decomposes at 690°C. The presence of fluorine in a Roman artefact is not too exotic, because fluorite (CaF_2 , which melts at

1360°C), is quite common in the surroundings of Rome, and it may occur in silver mines. Obviously the Romans were not aware of elemental chemistry, but we found that in modern metallurgy fluorite is used as flux, i.e. a substance mixed with a metal to promote melting. The Romans may have found it effective to mix fluorite with silver, just by trial and error, and the practice was then lost through history,

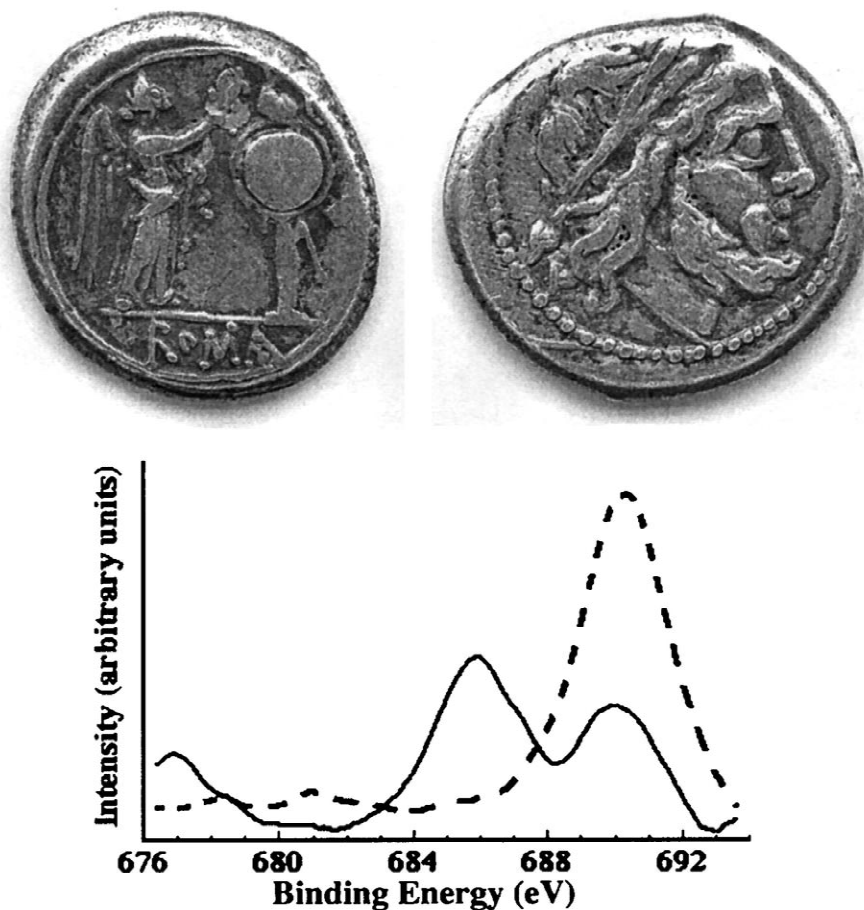


Fig. 3. Top: visible light microscopy images of the front and the back of the 211 B.C. Roman coin (diameter 9–12 mm) from the mint of Rome, found in La Molella (Sabaudia, Rome). Bottom: XPS spectra of Fluorine, obtained after Ar ion sputtering from the shield and the arm on the front of the coin. The two spectra show different oxidation states persisting after sputtering, probably due to uneven sputtering caused by the coin's topographic relief.

since there is no other reported evidence of F in Ag coins, either ancient or modern.

4. Conclusions

We explored the possibility of using X-PEEM spectromicroscopy in new fields, such as archaeology, geology and geomicrobiology. The experiments, initially conceived only as feasibility tests, demonstrated to be successful and delivered new insights in each one of these unusual fields. The most unexpected finding was that we could perform PEEM

of a 1-mm thick piece of rock. This result leads to the thought that it is not correct to exclude a PEEM experiment a priori because it does not seem feasible: the best approach is trying first, and then analyzing and interpreting the results.

Acknowledgements

We thank Marco Gioni and Fabian Zwick for the use of the ESCA machine at the EPFL, Jeff Cutler for his use of the XPS instrument at the Air Force Base in Ohio. We are indebted to Roger Hansen for

his broad knowledge in chemistry, and his generous sharing it with us. The spectromicroscopy experiments were performed under EPFL, FNRS and Italian CNR grants, at the Wisconsin Synchrotron Radiation Center, a facility supported by NSF under grant DMR-95-31009.

References

- [1] E. Bauer, *Ultramicroscopy* 36 (1991) 52.
- [2] B.P. Tonner, J.R. Harp, S.F. Koranda, J. Zhang, An electrostatic microscope for synchrotron radiation X-ray absorption microspectroscopy, *Rev. Sci. Instrum.* 63 (1992) 564.
- [3] G.F. Rempfer, O.H. Griffith, The resolution of photoelectron microscopes with UV, X-ray and synchrotron excitation sources, *Ultramicroscopy* 27 (1989) 273.
- [4] S. Anders, H.A. Padmore, R.M. Duarte, T. Renner, T. Stammer, A. Scholl, Photoemission electron microscope for the study of magnetic materials, *Rev. Sci. Instrum.* 70 (1999) 3973.
- [5] G. De Stasio, D. Dunham, B.P. Tonner, D. Mercanti, M.T. Ciotti, C. Coluzza, P. Perfetti, G. Margaritondo, Aluminum in rat cerebellar neural cultures, *Neuro Report* 4 (1993) 1175.
- [6] G. De Stasio, G. Margaritondo, Photoelectron spectromicroscopy with synchrotron radiation: applications to neurobiology, in: H. Ade (Ed.), *Spectromicroscopy with VUV Photons and X-Rays*, Special Issue of *J. Electr. Spectr. and Rel. Phenom.*, Elsevier, Amsterdam, 1997, p. 137.
- [7] B. Gilbert, L. Perfetti, O. Fauchoux, J. Redondo, P.-A. Baudat, R. Andres, M. Neumann, S. Steen, D. Gabel, D. Mercanti, M.T. Ciotti, P. Perfetti, G. Margaritondo, G. De Stasio, The spectromicroscopy of boron in human glioblastomas following administration of BSH, *Phys. Rev. E* 62 (2000) 1110.
- [8] G. De Stasio, B. Gilbert, T. Nelson, R. Hansen, J. Wallace, D. Mercanti, M. Capozzi, P.A. Baudat, P. Perfetti, G. Margaritondo, B.P. Tonner, Feasibility tests of transmission X-ray photoelectron emission microscopy (X-PEEM) of wet samples, *Rev. Sci. Instrum.* 71 (2000) 11.
- [9] G.W. Canning, M.L. Suominen Fuller, G.M. Bancroft, M. Kasrai, J.N. Cutler, G. De Stasio, B. Gilbert, Spectromicroscopy of tribological films from engine oil additives: part I: films from zddp's, *Tribology Letters* 6 (1999) 159.
- [10] J.N. Cutler, J.H. Sanders, P.J. John, G. De Stasio, B. Gilbert, K. Tan, Chemical characterization of antiwear films generated by *Tris*-[*p*-(perfluoroalkylether) phenyl phosphine using X-ray absorption spectroscopy, *WEAR* 236 (1999) 165.
- [11] H. Ade, D.A. Winesett, A.P. Smith, S. Anders, T. Stammer, C. Heske, D. Slep, M.H. Rafailovich, J. Sokolov, J. Stohr, Bulk and surface characterization of a dewetting thin film polymer bilayer, *Appl. Phys. Lett.* 73 (1998) 3775.
- [12] D.N. McIlroy, D. Zhang, R.M. Cohen, J. Wharton, Y. Geng, M.G. Norton, G. De Stasio, B. Gilbert, L. Perfetti, J.H. Streiff, B. Broocks, J.L. McHale, Electronic and dynamic studies of boron carbide nanowires, *Phys. Rev. B* 60 (1999) 4874.
- [13] M. Labrenz, G.K. Druschel, T. Thomsen-Ebert, B. Gilbert, S.A. Welch, K.M. Kemner, G.A. Logan, R.E. Summons, G. De Stasio, P.L. Bond, B. Lai, S.D. Kelly, J.F. Banfield, Sphalerite (ZnS) deposits forming due to growth of natural communities of sulfate-reducing bacteria, *Science*, (in press).
- [14] E. Bauer et al., this volume.
- [15] G. De Stasio, M. Capozzi, G.F. Lorusso, P.A. Baudat, T.C. Droubay, P. Perfetti, G. Margaritondo, B.P. Tonner, MEPHISTO: performance tests of a novel synchrotron imaging photoelectron spectromicroscope, *Rev. Sci. Instrum.* 69 (1998) 2062.
- [16] V. Kiryukhin, D. Casa, J.P. Hill, B. Keimer, A. Vigliante, Y. Tomioka, Y. Tokura, An X-ray-induced insulator-metal transition in a magnetoresistive manganite, *Nature* 386 (1997) 813.
- [17] B. Gilbert, R. Andres, P. Perfetti, G. Margaritondo, G. Rempfer, G. De Stasio, Charging phenomena in PEEM imaging and spectroscopy, *Ultramicroscopy* 83 (2000) 123.
- [18] J. Rothe, E.M. Kneedler, K. Pecher, B.P. Tonner, K.H. Nealson, T. Grundl, W. Meyer-Ilse, T. Warwick, Spectromicroscopy of Mn distributions in micronodules produced by biomineralization, *J. Synch. Rad.* 6 (1999) 359.
- [19] G. De Stasio, L. Perfetti, B. Gilbert, O. Fauchoux, M. Capozzi, P. Perfetti, G. Margaritondo, B.P. Tonner, The MEPHISTO spectromicroscope reaches 20 nm lateral resolution, *Rev. Sci. Instrum.* 70 (1999) 1740.
- [20] B. Gilbert, G. Margaritondo, S. Douglas, K.J. Nealson, R.F. Egerton, G.F. Rempfer, G. De Stasio, XANES microspectroscopy of biominerals with photoconducting charge compensation 114–116 (2001) 1005.
- [21] CRC Handbook of Chemistry and Physics, Chemical Rubber Company, Cleveland, OH, 44128.